AFRL-SN-WP-TP-2005-104

A MODEL FOR DIELECTRIC-CHARGING EFFECTS IN RF MEMS CAPACITIVE SWITCHES

Xiaobin Yuan, James C. M. Hwang, David Forehand, and Charles L. Goldsmith

MARCH 2005

Approved for public release; distribution is unlimited.

STINFO FINAL REPORT

SENSORS DIRECTORATE
AIR FORCE RESEARCH LABORATORY
AIR FORCE MATERIEL COMMAND
WRIGHT-PATTERSON AIR FORCE BASE, OH 45433-7320

NOTICE

Using Government drawings, specifications, or other data included in this document for any purpose other than Government procurement does not in any way obligate the U.S. Government. The fact that the Government formulated or supplied the drawings, specifications, or other data does not license the holder or any other person or corporation; or convey any rights or permission to manufacture, use, or sell any patented invention that may relate to them.

This report was cleared for public release by the Air Force Research Laboratory Wright Site Public Affairs Office (AFRL/WS) and is releasable to the National Technical Information Service (NTIS). It will be available to the general public, including foreign nationals.

THIS TECHNICAL REPORT IS APPROVED FOR PUBLICATION.

/s/

JOHN L. EBEL
Electron Devices Branch
Aerospace Components Division

/s/

KENICHI NAKANO, Chief
Electron Devices Branch
Aerospace Components Division

/s/

TODD A. KASTLE, Chief
Aerospace Components Division
Sensors Directorate

This report is published in the interest of scientific and technical information exchange and its publication does not constitute the Government's approval or disapproval of its ideas or findings.

REPORT DOCUMENTATION PAGE

Form Approved
OMB No. 0704-0188

1. REPORT DATE *(DD-MM-YY)*	2. REPORT TYPE	3. DATES COVERED *(From - To)*
March 2005	Conference Paper Preprint	08/23/2003 – 03/04/2005

4. TITLE AND SUBTITLE
A MODEL FOR DIELECTRIC-CHARGING EFFECTS IN RF MEMS CAPACITIVE SWITCHES

5a. CONTRACT NUMBER
F33615-03-C-7003

5b. GRANT NUMBER

5c. PROGRAM ELEMENT NUMBER
69199F

6. AUTHOR(S)
Xiaobin Yuan and James C. M. Hwang (Lehigh University)
David Forehand and Charles L. Goldsmith (MEMtronics Corporation)

5d. PROJECT NUMBER
ARPS

5e. TASK NUMBER
ND

5f. WORK UNIT NUMBER
AN

7. PERFORMING ORGANIZATION NAME(S) AND ADDRESS(ES)

Lehigh University
Bethlehem, PA 18015

MEMtronics Corporation
3000 Custer Road, Suite 270-400
Plano, TX 75075

8. PERFORMING ORGANIZATION REPORT NUMBER

9. SPONSORING/MONITORING AGENCY NAME(S) AND ADDRESS(ES)

Sensors Directorate
Air Force Research Laboratory
Air Force Materiel Command
Wright-Patterson AFB, OH 45433-7320

DARPA

10. SPONSORING/MONITORING AGENCY ACRONYM(S)
AFRL/SNDD

11. SPONSORING/MONITORING AGENCY REPORT NUMBER(S)
AFRL-SN-WP-TP-2005-104

12. DISTRIBUTION/AVAILABILITY STATEMENT
Approved for public release; distribution is unlimited.

13. SUPPLEMENTARY NOTES
Report contains color. To be published in the 2005 IEEE MTT-S International Microwave Symposium.

14. ABSTRACT

For the first time, charging and discharging of traps in the dielectric of state-of-the-art RF MEMS capacitive switches were characterized in detail. Densities and time constants of different trap species were extracted under different control voltages. It was found that, while charging and discharging time constants are relatively independent of control voltage, steady-state charge densities increase exponentially with control voltage. A charge model was constructed to predict the amount of charge injected into the dielectric and the corresponding shift in actuation voltage. The model was verified against the actuation-voltage shift under accelerated test conditions and found to be in good agreement with the experimental data. Both modeled and measured data suggested that the dielectric-charging effects can be accelerated by duty cycle and peak voltage of the actuation waveform.

15. SUBJECT TERMS
Charging, dielectric, lifetime, MEMS, RF, reliability, switch, trap

16. SECURITY CLASSIFICATION OF:			17. LIMITATION OF ABSTRACT:	18. NUMBER OF PAGES	19a. NAME OF RESPONSIBLE PERSON (Monitor)
a. REPORT	b. ABSTRACT	c. THIS PAGE			John L. Ebel
Unclassified	Unclassified	Unclassified	SAR	14	19b. TELEPHONE NUMBER *(Include Area Code)* (937) 255-1874 x3462

Standard Form 298 (Rev. 8-98)
Prescribed by ANSI Std. Z39-18

A Model for Dielectric-Charging Effects in RF MEMS Capacitive Switches

Xiaobin Yuan, *Student Member, IEEE,* James C. M. Hwang, *Fellow, IEEE,* David Forehand, *Member, IEEE,* and Charles L. Goldsmith, *Senior Member, IEEE*

***Abstract*—For the first time, charging and discharging of traps in the dielectric of state-of-the-art RF MEMS capacitive switches were characterized in detail. Densities and time constants of different trap species were extracted under different control voltages. It was found that, while charging and discharging time constants are relatively independent of control voltage, steady-state charge densities increase exponentially with control voltage. A charge model was constructed to predict the amount of charge injected into the dielectric and the corresponding shift in actuation voltage. The model was verified against the actuation-voltage shift under accelerated test conditions and found to be in good agreement with the experimental data. Both modeled and measured data suggested that the dielectric-charging effects can be accelerated by duty cycle and peak voltage of the actuation waveform.**

***Index Terms*—Charging, dielectric, lifetime, MEMS, RF, reliability, switch, trap.**

I. Introduction

RF MEMS is an emerging technology for low loss switching, reconfigurable network and phase shifter applications [1]-[4]. However, commercialization of RF MEMS devices is hindered by a number of factors such as reliability and packaging. In particular, the lifetime of electrostatically actuated RF MEMS capacitive switches is limited by dielectric-charging effects [5]. The dielectric is typically low-temperature deposited silicon dioxide or nitride with a high density (10^{18} /cm^3) of traps associated with silicon dangling bonds. During switch operation, the electric field across the dielectric can be as high as 10^6 V/cm causing electrons to be injected into the switch dielectric and become trapped. With repeated operation, charge gradually builds up in the dielectric which will change the electrostatic force on the switching membrane resulting in actuation-voltage shift and/or stiction [6].

To date, dielectric-charging effects in RF MEMS devices have been studied by different research groups [5]-[9] and a general charge model was proposed in the literature [9]. However, there has been no effort to experimentally extract the charge model parameters and accurately model the charging state of the dielectric and its impact on actuation voltage. Moreover, the acceleration of charging effects by different actuation waveforms has not been studied in detail. Using a special test structure and setup, we directly characterized charging and discharging transient currents in state-of-the-art RF MEMS capacitive switches and constructed a simple charge model to predict charging effects on the operation of the switches under different control voltages [10]. This paper expands on [10] to include the model prediction of charge injection under different actuation-waveform frequencies, peak voltages and duty cycles which was verified by the experimental data. It was experimentally observed and theoretically confirmed by the model that the charging effects can be accelerated by increasing the peak voltage or duty cycle of the actuation waveform.

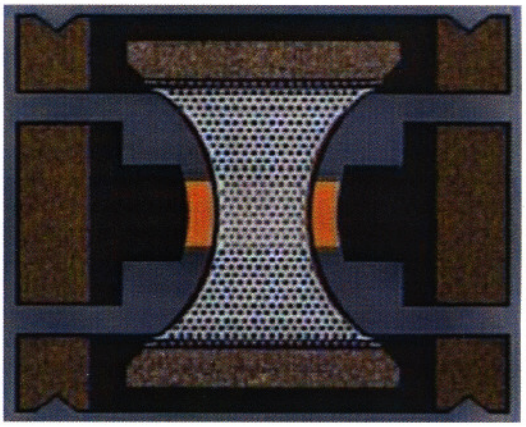

Fig. 1. Top view of a state-of-the-art RF MEMS capacitive switch.

II. Experimental

A. Device Structure

Fig. 1 illustrates a state-of-the-art metal-dielectric-metal RF MEMS capacitive switch fabricated on a glass substrate. The dielectric is sputtered silicon dioxide with a thickness of 0.25 μm and a dielectric constant of 4.0. The top electrode is a 0.3-μm-thick flexible aluminum membrane that is grounded.

Manuscript submitted on November 18, 2004. Work was partially supported by the Air Force Research Laboratory under Contract No. F33615-03-C-7003. The contract was funded by the Defense Advanced Research Projects Area (DARPA) under the Harsh Environment, Robust Micromachined Technology (HERMIT) program.

X. Yuan and J. C. M. Hwang are with Lehigh University, Bethlehem, PA 18015 USA. X. Yuan can be contacted at (610) 758-5109 or xiy2@lehigh.edu.

D. Forehand and C. Goldsmith are with MEMtronics Corp., Plano, TX 75075 USA.

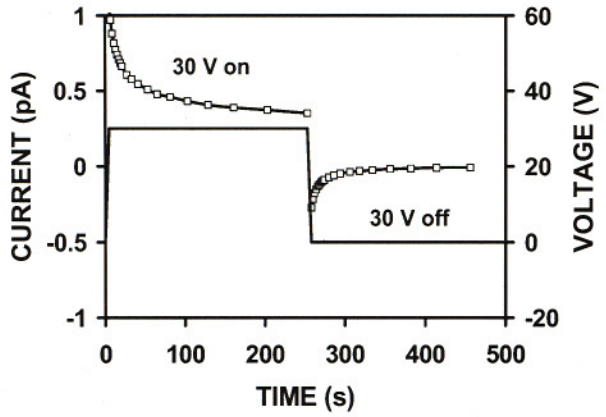

Fig. 2. Measured charging current under 30 V and discharging current after removal of the voltage on an MIM test structure. Solid line is the control voltage waveform.

The bottom chromium/gold electrode serves as the center conductor of a 50 Ω coplanar waveguide for the RF signal. Without any electrostatic force, the membrane is normally suspended in air 2.5 μm above the dielectric. Control voltage in the range of 25-35 V is applied to the bottom electrode, which brings the membrane in contact with the dielectric thus forming a 120 μm x 80 μm capacitor which will shunt the RF signal to ground. When the control voltage is removed, the membrane is supposed to spring back to its fully suspended position, resulting in little capacitive load to the RF signal. The switch has low insertion loss (0.06 dB) and reasonable isolation (15 dB) at 35 GHz. The switching time is less than 10 μs. Details of the design, fabrication and performance of the switch will be reported elsewhere.

B. Transient Current Measurements

In order to quantitatively characterize the trap states of the dielectric, charging and discharging current transients [11] were measured on switches whose membrane was intentionally fabricated in a permanently down position (without the sacrificial release layer) thus resembling a metal-insulator-metal capacitor. A precision semiconductor parameter analyzer was used to force a voltage pulse onto the switch while sensing the current transient. Well-guarded probe station and probes were used to suppress the capacitive and leakage currents in the measurement path, thus extending the transient current measurement range below pA level.

As shown in Fig. 2, when a voltage pulse is applied to a permanently down switch, the total current includes displacement current, trap charging current, and steady-state leakage current. After this voltage is removed, charges accumulated on the electrodes (capacitor charge) and the dielectric (trap charge) begin to discharge. Since the time constant for the displacement current is of the order of milliseconds, the current transients shown in Fig. 2 comprise mainly trap charging and discharging currents. In this case, trap

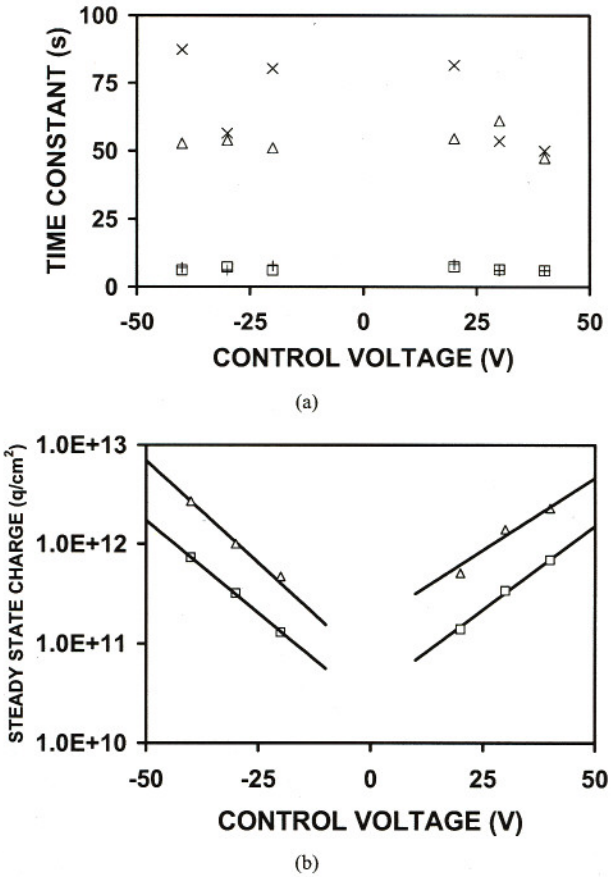

Fig. 3. (a) Trap 1 (□) charging and (+) discharging and trap 2 (Δ) charging and (x) discharging time constants and (b) (symbols) extracted and (lines) fitted steady-state charge density for (□) trap 1 and (Δ) trap 2 under -40, -30, -20, 20, 30 and 40 V. The time constants show no significant bias dependence whereas the steady-state charge density is exponentially dependent on the control voltage.

density and charging/discharging time constants can be extracted for different trap species.

C. Accelerated Charging Tests

The accelerated charging tests for the switches were performed using the time-domain switch characterization setup [5], [6]. The input RF signal (a 6 GHz, 10 dBm sinusoidal signal) was applied to the switch input port together with the actuation waveform. The RF output was sensed by using a 26.5 GHz diode detector. Both the actuation and output waveforms were monitored by using an oscilloscope. First, a saw-tooth actuation waveform (0 to -30 V) was applied to a pristine switch to sense the pre-stress actuation voltage. Then stressing of the switch was performed by applying a square-wave signal as the actuation waveform for different time periods. After each stressing period, another saw-tooth actuation waveform was applied to the switch to sense the post-stress actuation voltage. Thus, the actuation-voltage shift for the stressing period can be determined. Frequency, duty cycle, and peak voltage of the square-wave actuation waveform were varied to study the acceleration factor for the dielectric-charging effects.

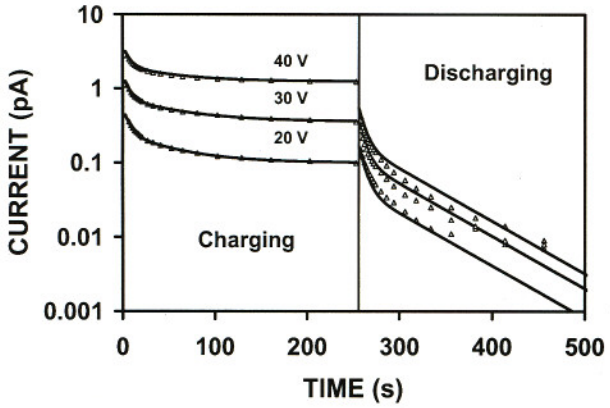

(a)

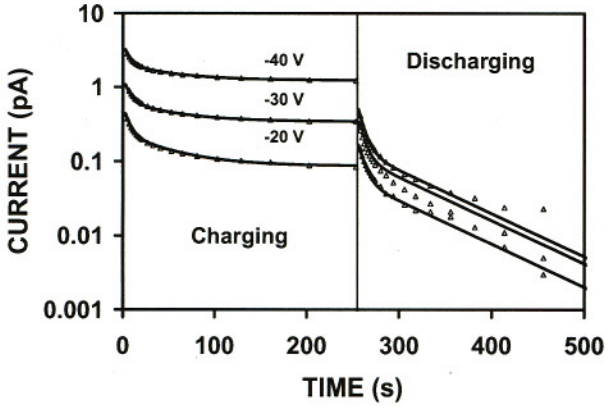

(b)

Fig. 4. Absolute values of (symbols) measured and (lines) calculated charging and discharging current transients under (a) positive and (b) negative control voltages.

III. Model Construction

The injected charge density in the dielectric is modeled as

$$Q = \sum_J Q^J [1 - \exp(-t_{ON} / \tau_C^J)] \exp(-t_{OFF} / \tau_D^J) \quad (1)$$

where Q^J is the steady-state charge density of the *Jth* specie of trap, τ_C and τ_D are the charging and discharging time constants, t_{ON} and t_{OFF} are the on and off times of the switch corresponding to the charging and discharging times.

Assuming all traps are empty before applying the charging voltage pulse, current transient due to charging of the trap states after the voltage is applied is

$$I_C = qA\frac{dQ}{dt} = qA\sum_J \frac{Q^J}{\tau_C^J} \exp(-t_{ON} / \tau_C^J) \quad (2)$$

where q is the electron charge and A is the surface area of the dielectric. Similarly, assuming the traps are all charged during the voltage pulse duration, current transient due to the discharging of the trap states after removal of the voltage is

$$I_D = qA\frac{dQ}{dt} = -qA\sum_J \frac{Q^J}{\tau_D^J} \exp(-t_{OFF} / \tau_D^J) \quad (3)$$

TABLE I
EXTRACTED MODEL PARAMETERS

Positive Bias				
J	τ_C (s)	τ_D (s)	Q_0 (cm^{-2})	V_0 (V)
1	6.6	6.8	3.1×10^{10}	12.9
2	54.3	61.6	1.6×10^{11}	14.9
Negative Bias				
J	τ_C (s)	τ_D (s)	Q_0 (cm^{-2})	V_0 (V)
1	6.5	7.0	2.4×10^{10}	11.7
2	52.5	74.7	6.0×10^{10}	10.5

Switch lifetime has exhibited an exponential dependence on the control voltage [5], implying that either the charge density or the time constant is strongly dependent on voltage. To investigate the voltage dependence of the model parameters, charging and discharging currents were measured on permanently down switches under control voltages both above and below the actuation voltage of normal switches. Then the model parameters (Q^J, τ_C and τ_D) were extracted for each voltage value by fitting the current transients with exponential functions such as in (2) and (3). Two exponential functions, representing two trap species, were found to give good fit.

As shown in Fig. 3(a), the extracted charging and discharging time constants for both positive and negative control voltages exhibit no strong voltage dependence. Therefore, τ_C and τ_D were taken as the average of the time constants extracted under different voltages. By contrast, the steady-state charge density is found to vary exponentially with the control voltage, as illustrated in Fig. 3(b). The voltage dependence of the steady-state charge density for the *Jth* trap is modeled as

$$Q^J = Q_0^J \exp(V / V_0^J) \quad (4)$$

where V is the applied voltage whereas Q_0 and V_0 are fitting parameters.

Using the above-described approach, two sets of model parameters were extracted for positive and negative control voltages as listed in Table I. The measured and calculated transient charging and discharging currents under different control voltages are plotted in Fig. 4 showing good agreement between experimental data and theoretical calculation.

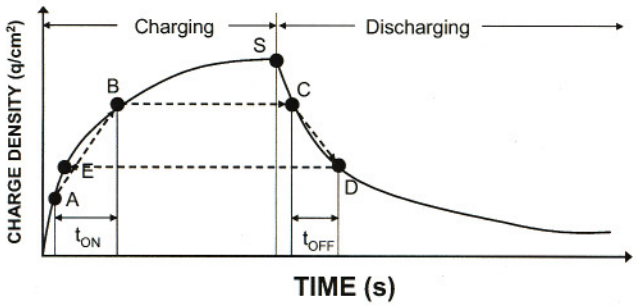

Fig. 5. Illustration of charge calculation under a square-wave actuation waveform. t_{ON} and t_{OFF} are the on and off times of the switch. After one operation cycle, charge density increases from the initial state A to the end state B.

IV. Model Verification And Charge Acceleration

A. Theoretical Calculation

The model parameters in (1) and (4) were extracted with very long charging and discharging times so that traps were all empty before charging and all filled before discharging, as illustrated in Fig. 5 by a charging curve that starts from the origin and ends in saturation (State S). The charging and discharging curves are expressed as follows:

$$Q = \sum_J Q^J [1 - \exp(-t_{ON} / \tau_C^J)] \tag{5}$$

$$Q = \sum_J Q^J \exp(-t_{OFF} / \tau_D^J) \tag{6}$$

During real switch operation under square-wave actuation waveform, the initial charging state at the beginning of each operating cycle will be somewhere between empty and full, such as State A on the charging curve. After the switch is turned on, the charging state moves higher to State B during the on time of the switch. After the switch is turned off, the dielectric starts to discharge from State C on the discharging curve, which is mapped from State B of the charging curve. After certain off period of the switch, the dielectric is discharged to State D, which is then mapped back to State E on the charging curve, indicating the cumulative effect of one charging/discharging cycle is to move the initial state from A to E. Thus, the model repeats itself in such a ratchet fashion until the desired number of cycles has been operated. The model has four input parameters: peak voltage, number of operating cycles, on time, and off time of the switch. Changing the input peak voltage will affect the steady-state charge density as predicted by (4). Different on and off times determine the frequency and duty cycle of the square-wave actuation waveform.

The actuation-voltage shift due to dielectric charging can be expressed as

$$\Delta V = qhQ / \varepsilon_0 \varepsilon_r \tag{7}$$

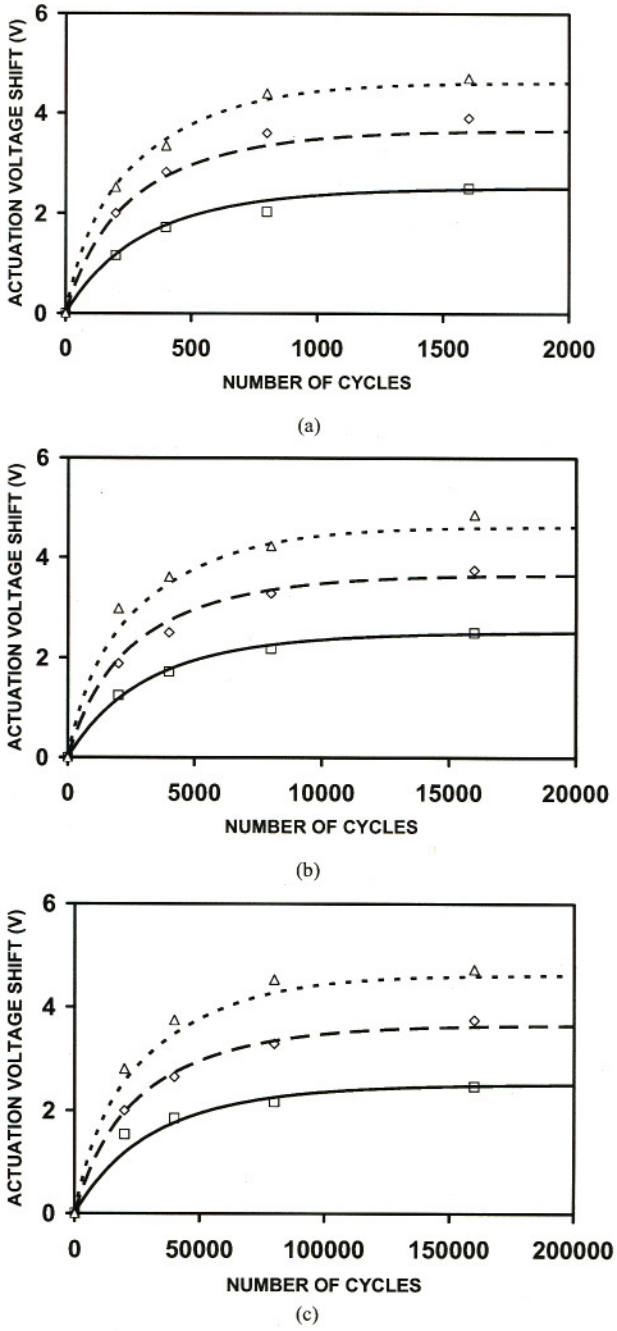

Fig. 6. Actuation-voltage shift as a function of operating cycles. The stress signal is a 0 to -30 V square wave with three frequencies: (a) 10 Hz, (b) 100 Hz, and (c) 1 KHz. Modeled actuation-voltage shift for (—) 25%, (- - -) 50%, and (· · ·) 75% square-wave duty cycles. Measured actuation-voltage shift for (□) 25%, (◊) 50%, and (Δ) 75% square-wave duty cycles. Stress time was the same (20 s, 40 s, 80 s, and 160 s) for all three frequencies. h was set to 110 nm for model calculation. Both modeled and measured data show that charge injection is accelerated by increasing the duty cycle.

where h is the distance between the bottom electrode and the trapped charge sheet, Q is the injected charge density calculated by the above-described routine, ε_0 is the permittivity of free space, and ε_r is the relative dielectric constant of the switch

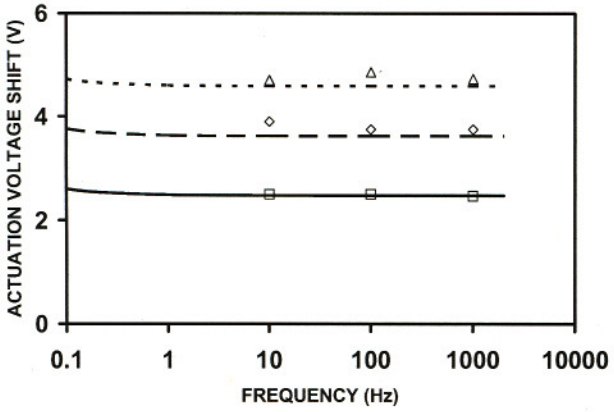

Fig. 7. Actuation-voltage shift as a function of stress signal frequency. The stress signal is a -30 V, 160 s long square wave. Measurements were taken at 10 Hz, 100 Hz, and 1 KHz square-wave frequencies. Modeled results for (—) 25%, (- - -) 50%, and (· · ·) 75% square-wave duty cycles. Measured results for (□) 25%, (◊) 50%, and (Δ) 75% square-wave duty cycles. *h* was set to 110 nm for model calculation. Both modeled and measured data show little frequency dependence above 1 Hz.

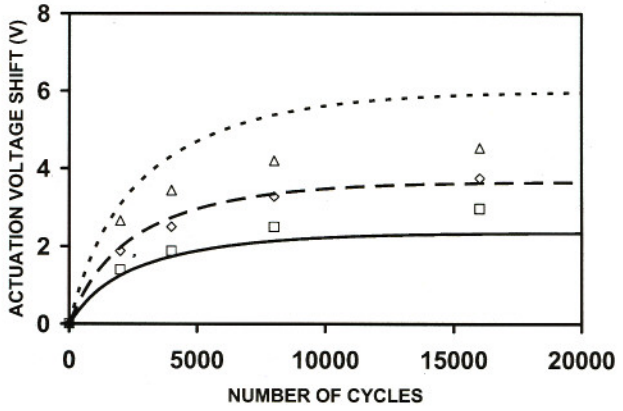

Fig. 8. Actuation-voltage shift as a function of operating cycles and stress voltages. The stress signal is a 50% duty cycle, 100 Hz square wave. Modeled results for (—) -25 V, (- - -) -30 V, and (· · ·) -35 V square-wave peak voltages. Measured results for (□) -25 V, (◊) -30 V, or (Δ) -35 V square-wave peak voltages. *h* was set to 110 nm for model calculation. Both modeled and measured data show that charge injection is accelerated by increasing the peak voltage of the square wave.

dielectric. The actuation-voltage shift for certain stress period is predicted by (7) with *h* optimized to give the best fit between model prediction and experimental data. The model was verified against different square-wave frequencies, duty cycles and peak voltages.

B. Duty Cycle Acceleration

The amount of charge injected within one operation cycle is determined by three parameters: peak voltage, duty cycle, and frequency of the square-wave actuation waveform. Since duty cycle and frequency are the parameters that determine the on and off time of the switch, their effects on dielectric charging were investigated at the same time. The actuation-voltage shift under different frequencies and duty cycles were measured. The square-wave signal used to stress the device has an "on" voltage of -30 V to charge the dielectric and an "off" voltage of 0 V to discharge the dielectric. The actuation voltage of the pristine switch is around -22 V hence -30 V is enough to actuate the device. The switch was operated at three different frequencies (10 Hz, 100 Hz, and 1 KHz). At each frequency, three duty cycles (25%, 50%, and 75%) were used to study the effect of different on and off times on the charging problem.

After applying the 0 to -30 V square-wave signal on the bottom electrode of the switch for certain period, actuation voltage was shifted to the positive direction indicating injection of negative charges from the bottom electrode into the dielectric. *h* was set to 110 nm (about half of the dielectric thickness) to give the global optimum fit between modeled and measured actuation-voltage shift for all three frequencies. Fig. 6 shows measured and modeled actuation-voltage shift against operating cycles. Both modeled and measured data suggest that for a fixed square-wave duty cycle, charge injection and actuation-voltage shift depend strongly on the total stress time instead of number of cycles operated (the maximum stress time showed in Fig. 6 is 200 s corresponding to 2000, 20000, and 200000 cycles for the three frequencies). Hence, within the frequency range used for the stress measurements (10 Hz to 1 KHz), charge injection during certain time duration has no obvious dependence on the stress frequency. On the other hand, increasing the square-wave duty cycle accelerates the dielectric-charging effects (increases the actuation-voltage shift) for all three frequencies as shown in Fig. 6.

Duty cycle acceleration of the charging effects makes immediate sense since for a fixed frequency, the charging and discharging time of the switch within one operating cycle is determined by the duty cycle of the square wave. For the extreme case of a dc stress (100% duty cycle), the charge density within the dielectric will increase from 0 to the saturated value (State S) on the charging curve as shown in Fig. 5. If the duty factor is extremely low (e.g., 0.01%), the charges accumulated during the on time of the switch will always be discharged completely in the off time before the next switching cycle starts, hence the charge density will stay around the origin in Fig. 5 no matter how many cycles are operated. An intermediate duty cycle (e.g., 50%) will cause the charge density to start from 0 and reach a saturated state some where below the State S when the charging and discharging processes reach equilibrium. Thus, the normally quoted number of cycles operated before failure is not a good figure of merit for RF MEMS capacitive switches whose lifetime is limited by the charging effects. Instead, switching frequency and waveform duty cycle (for square wave) must be well defined to obtain a fair comparison of the switch lifetimes.

C. Frequency Dependence

It was mentioned in the previous section that charge induced actuation-voltage shift has little frequency dependence (within 10 Hz to 1 KHz range) for a fixed stress time duration. Fig. 7 shows the actuation-voltage shift as a function of frequency. For 160 s of a 0 to -30 V square-wave stress, both modeled and

measured data confirmed the stress frequency independence within the frequency range used in the measurements (10 Hz to 1 KHz). However, as the frequency goes below 1 Hz, the modeled actuation-voltage shift starts to increase from its high frequency value. This is because as the frequency approaches inverse of the stress time (1/160), duty cycle of the square wave becomes meaningless for the stress time duration (e.g., a 0.003125 Hz, 50 % duty cycle, 0 to -30 V square-wave signal has a 160 s on time, hence during the 160 s stress duration, there is always a -30 V bias applied on the switch resembling a dc stress condition that accelerates charge injection.).

D. *Voltage Acceleration*

It has been shown that increasing the actuation waveform voltage will accelerate the charge injection and shorten the switch lifetime [5]. Voltage acceleration of the charging effects was studied by using different square-wave peak voltages (-25 V, -30 V, and -35 V) to stress the switch and record the corresponding actuation-voltage shift. The stress signal is a 100 Hz, 50% duty cycle square wave. Both modeled and measured data shown in Fig. 8 confirmed the fact that increasing the square-wave peak voltage accelerates charge injection hence increases actuation-voltage shift. Since the peak voltage will only affect the steady-state charge density instead of charging/discharging time constants as shown in Fig. 3, similar voltage acceleration results should be expected for other stress frequencies and duty cycles.

V. Discussion

Although the present model assumes that the injected charge is an equivalent sheet of charge 110 nm above the bottom electrode, the actual bottom-injected electrons most likely are distributed across the thickness of the dielectric. Since their collective effect on the actuation voltage can be approximated by a sheet charge, it greatly simplifies the model making it possible to predict the dielectric-charging effect under complicated actuation waveforms. In addition, tunneling and trap-to-trap hopping were not taken into account in the present simple model so that (1)-(3) are only based on the first-order carrier capture and emission dynamics. Therefore, the extracted charging and discharging time constants should not be construed as exact capture and emission times of the traps.

The current transients measured on the permanently down switches were used to predict the dielectric-charging effects in functioning switches. Although charge injection from the bottom electrode is expected to be similar in both cases, charge injection from the top electrode can be rather different due to the non-ideal contact between the top electrode and the dielectric in functioning switches. For the present switches and bias conditions (negative voltage on the bottom electrode), the dielectric-charging effect is dominated by charge injection from the bottom so that any difference in charge injection from the top can be ignored. This may not be the case in other switches or bias conditions for which charge injection from the top is not negligible (e.g., negative bias applied on the top electrode causing electron injection from the top).

For RF MEMS capacitive switches whose lifetime is limited by the dielectric-charging effects, the analysis in the previous section shows that number of cycles operated before failure is not a good reliability measure. As shown by the modeled and measured data in Fig. 6 and Fig. 8, duty cycle and voltage are the acceleration factors for the charging effects. Hence the desirable bias waveform to minimize the charging effects should have the following characteristics: high frequency, low peak voltage, and low duty cycle. The idea is to reduce the time that the switch spent in the "on" state with high voltage across the dielectric while increase the "off" state duration to help discharge the traps. Switching frequency, waveform duty cycle and peak voltage (for square wave) must be well defined to obtain a fair comparison of the switch lifetimes.

A dual-pulse waveform has been proposed to minimize the charging effects [5] where a short high voltage pull-down pulse (50 μs) was used to pull down the switching membrane quickly and a much lower voltage was used to hold the membrane down for the rest of the on time of the switch. Thus, a low duty cycle dual-pulse waveform, which is capable of minimizing the charge acceleration by duty cycle and voltage as shown in Fig. 6 and Fig. 8, is the ideal candidate if unipolar actuation waveform is used to drive the switch. Comparing to unipolar waveforms, bipolar actuation waveforms have been proved to be a better solution to prevent charge accumulation in the dielectric where the discharging of the traps is facilitated by the ensuing voltage pulse whose polarity is opposite to the previous charging pulse [8], [12]. However, the charging and discharging dynamics are more complex than the unipolar case and can not be taken care of by the present charge model.

VI. Conclusion

Charging and discharging currents of traps in permanently down RF MEMS capacitive switches were measured. Based on the measured data, a simple charge model was extracted. The steady-state charge density was found to have an exponential dependence on the control voltage while the charging and discharging time constants were relatively independent of voltage. The model is used to predict the actuation-voltage shift under accelerated test conditions and found to be in good agreement with the experimental data. Effects of square-wave stress frequency, duty cycle, and voltage on the charging problem were analyzed using the model and validated experimentally. Duty cycle and peak voltage of the square-wave actuation waveform were found to be the acceleration factors for the charging effects. Frequency showed little effect on charging within the range of 10 Hz to 1 KHz. Once the acceleration factors for the charging problem were studied, the model can be used as a theoretical tool to help design a favorable actuation waveform to minimize dielectric-charging effects in RF MEMS capacitive switches.

REFERENCES

[1] C. Goldsmith, Z. Yao, S. Eshelman, and D. Denniston, "Performance of low-loss RF MEMS capacitive switches," *IEEE Microwave and Guided Wave Lett.*, vol. 8, no. 8, pp.269-271, Aug. 1998.

[2] D. Peroulis, S. Pacheco, and L. P. B. Katehi, "MEMS devices for high isolation switching and tunable filtering," in *2000 IEEE MTT-S Int. Microwave Symp. Dig.*, June 2000, pp. 1217-1220.

[3] A. Malczewski, S. Eshelman, B. Pillans, J. Ehmke, and C. Goldsmith, "X-band RF MEMS phase shifters for phased array applications," *IEEE Microwave and Guided Wave Lett.*, vol. 9, no. 12, pp.517-519, Dec. 1999.

[4] B. Pillans, S. Eshelman, A. Malczewski, J. Ehmke, and C. Goldsmith, "Ka-band RF MEMS phase shifters," *IEEE Microwave and Guided Wave Lett.*, vol. 9, no. 12, pp.520-522, Dec. 1999.

[5] C. Goldsmith, J. Ehmke, A. Malczewski, B. Pillans, S. Eshelman, Z. Yao, J. Brank, and M. Eberly, "Lifetime characterization of capacitive RF MEMS switches," in *2001 IEEE MTT-S Int. Microwave Symp. Dig.*, 2001, pp. 227-230.

[6] X. Yuan, S. V. Cherepko, J. C. M. Hwang, C. L. Goldsmith, C. Nordquist, and C. Dyck, "Initial observation and analysis of dielectric-charging effects on RF MEMS capacitive switches," in *IEEE MTT-S Int. Microwave Symp. Dig.*, June 2004, pp. 1943-1946.

[7] W. M. van Spengen, R. Puers, R. Mertens, and I. De Wolf, "Experimental characterization of stiction due to charging in RF MEMS," *in Proc. IEEE Electron Devices Meeting*, 2002, pp. 901-904.

[8] J. R. Reid, and R. T. Webster, "Measurements of charging in capacitive microelectromechanical switches," *Electron. Lett.*, vol. 38, no. 24, Nov. 2002.

[9] W. M. van Spengen, R. Puers, R. Mertens, and I. De Wolf, "A comprehensive model to predict the charging and reliability of capacitive RF MEMS switches," *J. Micromech. Microeng.*, vol. 14, pp. 514-521, Jan. 2004.

[10] X. Yuan, J. C. M. Hwang, D. Forehand, and C. L. Goldsmith, "Modeling and Characterization of Dielectric-Charging Effects in RF MEMS Capacitive Switches," to be published in *IEEE MTT-S Int. Microwave Symp. Dig.*, June 2005.

[11] H. Matsuura, M. Yoshimoto and H. Matsunami, "Discharging current transient spectroscopy for evaluating traps in insulators," *Jap. J. Appl. Phys.*, vol. 34, pp. L185-L187, Feb. 1995.

[12] G. M. Rebeiz, *RF MEMS Theory, Design, and Technology*, New Jersey: John Wiley & Sons, 2003, pp. 186-190.